Roton propagation and phonon-roton scattering in He II

V. Narayanamurti and R. C. Dynes
Bell Laboratories, Murray Hill, New Jersey
(Received 11 August 1975)

The propagation characteristics of high-energy excitations in He II are studied as a function of pressure, temperature, and frequency by means of a superconducting Sn fluorescent generator and a Sn tunnel detector and time-of-flight techniques. At saturated vapor pressure and low temperatures ($T \approx 0.1$ K) and with the detector energy gap possessing its full value (~ 14 K), a single well-defined pulse is observed to arrive at a time corresponding to that expected for the first echo (three traverses of the cell) of a low-energy phonon. This "echo pulse" disappears as the pressure is raised to 10 ± 2 bar and one observes a driven roton second sound at higher pressures. The echo pulse is interpreted as arising from a collinear interaction near the detector of a low-energy phonon with "fast" rotons (group velocity approximately equals the sound velocity c_0) by means of a three-particle interaction (phonon + roton → roton) first suggested by Pitaevskii. The data indicate that this Pitaevskii process turns off at high pressures and only the four-particle process (phonon + roton → phonon + roton) remains. With increasing magnetic field on the detector, ballistic phonons are observed as expected. The scattering of these ballistic phonons and a cloud of rotons are probed by means of a novel double-pulse technique and provides strong evidence for the existence of this collinear three-particle interaction at low pressures.

I. INTRODUCTION

The details of the shape of the excitation spectrum in He II and the implications for scattering processes have been the subject of much experimental and theoretical study.[1] The question as to whether the phonon portion of the excitation spectrum curves upward thus allowing three-phonon scattering processes[2] has been resolved only recently.[3] Studies of the roton-roton interaction possibly leading to a two-roton bound state have been the subject of intensive experimental[4] and theoretical[5] investigation. The subject of phonon-roton scattering has been investigated using various techniques, for example, the heat-pulse technique[6] and neutron scattering,[7] but as yet a clear picture of the scattering processes and the pressure dependences of these scattering processes has not emerged. In particular, several years ago Pitaevskii[8] pointed out that if the group velocity ($v_g = d\omega/dk$) of the rotons reaches the sound velocity c_0, the rotons can emit a phonon in a collinear process in analogy to the Cherenkov effect. This then implied that the roton lifetime should become substantially shorter for this three-particle process. At saturated vapor pressure (SVP), neutron scattering results suggested that there was indeed a region in q where $d\omega/dk \geq c_0$, thus allowing this process. Attempts to measure roton linewidths by neutron scattering[7] in this region of q in an effort to observe the turn on of this Pitaevskii scattering process were, however, unsuccessful. In addition, the pressure profoundly influences the shape of the excitation spectrum (both the phonon and roton branches) and the pressure dependence of this process is also unclear. High-pressure, neutron scattering data[1] suggest that the $v_g = c_0$ criterion is no longer met and this scattering process must therefore turn off at some intermediate pressure value.

In this paper, we describe a series of experiments to investigate the propagation of rotons and the roton-phonon interaction, including this Pitaevskii process. The experiments are pulsed time-of-flight measurements of phonons and rotons injected into the He II using a Sn flourscent generator[9] and detected after propagating a macroscopic distance by means of a Sn tunnel detector. An earlier preliminary report of one aspect of this work in very high magnetic fields, where the detectors behave as heat-pulse detectors, has already been published. There it was reported that at high pressures and intermediate temperatures a new propagating mode, roton second sound,[10] was observed. Here we extend these measurements to low values of the magnetic field (where the detector behaves as a quantum detector) and over various pressures and temperatures.

The plan of the paper is as follows. In Sec. II we describe briefly the experimental arrangement and then the results of a series of experiments as a function of pressure, temperature, applied magnetic field, and injector power. All of these variables have a strong influence on the phonon and roton numbers launched and detected in these experiments. In Sec. III we present a model, incorporating the earlier ideas of Pitaevskii and subsequent investigators[11] to describe our data. In this section we

will show that the three-particle process is consistent with these results and that at intermediate pressures, as the neutron scattering results imply, the process turns off. In Sec. IV we describe a series of scattering experiments to test this model and to determine quantitatively the pressure region over which this criterion of $v_g = c_0$ is satisfied. Finally, we present some numerical estimates of the scattering rates determined in these experiments and we draw some conclusions.

II. EXPERIMENTAL DESCRIPTION AND RESULTS

The experiments reported in this paper were performed in a dilution refrigerator using pulsed time-of-flight techniques, the details of which have been reported previously.[6] For phonon and roton generators and detectors, a thin-film Sn fluorescor and Sn-I-Sn tunnel junction, respectively, were used. The details of these quasimonochromatic devices have been described in detail elsewhere[9] and we emphasize here simply that the tunnel-junction detectors respond only to excitations whose energies $\hbar\omega$ are $\geq 2\Delta$ the energy gap of the superconductor. Excitations with energies less than 2Δ are not detected. The energy gap of Sn at low temperatures and zero applied magnetic field is $2\Delta = 1.20$ meV $= 13.95$ K. The Sn films were ≈ 600 Å thick and hence the energy gap $\Delta(H)$ could be tuned down from its maximum value by the application of a magnetic field parallel to the films. Care was taken to ensure the parallelicity of the applied field and the I-V characteristics of the tunnel junction were used as an operational measure of the amount of flux penetrating the films due to a transverse component of the field.

The tunnel junctions typically had a normal-state resistance of 10^{-2} Ω, and typical I-V traces, including traces taken in various fields up to the critical field of the film at 0.1 K, are shown in Fig. 1. From this series of curves, we observe the following points. First, the junctions used are of quite high quality, with a leakage current due to other transport processes down by several orders of magnitude from the tunneling current [Fig. 1(a)]. This high quality is necessary as otherwise the sensitivity of the junctions to excited quasiparticles at reduced temperatures

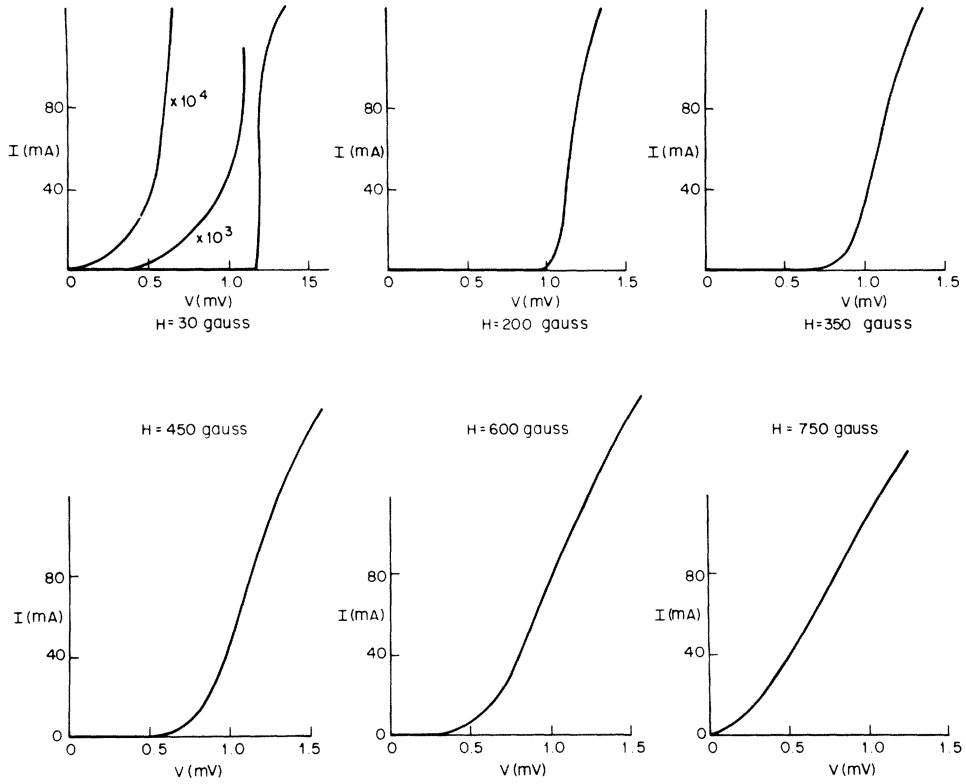

FIG. 1. I-V characteristics for a thin-film (~600 Å) Sn-I-Sn detector junction at 0.1 K. At low fields (30 G) the leakage rate due to other conduction mechanisms is $\lesssim 10^{-4}$ of the tunneling current. At higher fields, $\Delta(H)$ broadens but low-voltage currents are still low until the highest fields.

($T \ll T_c$) diminishes as other transport mechanisms dominate. This high quality (and film uniformity) was achieved in part by depositing the films onto glass substrates held at 77 K. Also notable in Fig. 1 is the fact that, as H is increased, the energy gap broadens substantially and the sharp square-root singularity which describes the gap edge of a BCS superconductor no longer exists. This is not a crucial factor in the conclusions drawn in this experiment but it is evident that the energy gap $\Delta(H)$ becomes somewhat less well defined at higher fields. Whether one defines the energy gap as the point of maximum slope in the I-V characteristic or the point in voltage where current begins to flow is a somewhat moot point as the sensitivity or the response of the junction is changing throughout this energy range. Our choice is to define $\Delta(H)$ as the point in voltage where appreciable current flows on the scale of Fig. 1. At any rate, for the conclusions drawn in this paper, this is not a crucial point. Finally, it is also evident from Fig. 1 that the amount of flux trapped in the films owing to a transverse field component is small. This is evidenced by the fact that for intermediate field values, there is no apparent enhancement of the current at very low voltages and only the reduction of the gap $\Delta(H)$ is measured.

Fortunately, for these experiments we have as a guide the excitation spectra $E(k)$ as measured by inelastic neutron scattering,[1] and these are shown at SVP and a pressure of 25.2 bar in Fig. 2. Also shown on this curve is the value $2\Delta_0$ of the full gap of superconducting Sn to show the energy threshold for detection. The generated spectrum, of course, will have a peak in its distribution at $2\Delta_0$ but will also have excitations at lower energies. It is seen from Fig. 2 that $2\Delta_0$ is close to the maximum of the phonon branch and intersects the positive branch of the roton part of the excitation spectrum. As $2\Delta_0$ is lowered with field, it will of course intersect the excitation spectrum at several points.

The experimental results which originally stimulated this investigation are shown in Fig. 3. Here we show photographs of pulsed time-of-flight measurements of signal as a function of time detected at the detector 2.34 mm from the generator at SVP and 24 bar, and taken at a temperature $T = 0.25$ K. These two pressures correspond approximately to the pressures where the $E(k)$ have been measured (Fig. 2). The arrows labeled τ_B and $3\times\tau_B$ are the points in time where phonons propagating at the sound velocity arrive at the detector (original signal and echo). Phonons (and rotons) with a lower group velocity v_g will, of course, arrive later than this. There are several interesting and puzzling aspects of this data worth noting. First, as expected from Fig. 2, we do not detect any signal arriving at τ_B as our detectors are not sensitive to phonons of that velocity. Figure 2 suggests, however, that in the roton branch $v_g(2\Delta_0) \approx c_0$ and since we detect no signal at τ_B we must conclude that either these excitations are short-lived, or our generators or detectors do not couple to them. We will see shortly that the former is the case.

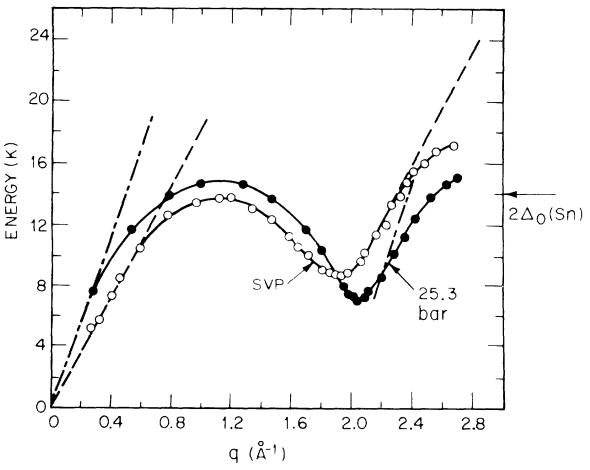

FIG. 2. $E(k)$ relation for He II at SVP and 25.3 bar. These curves were measured by inelastic neutron scattering and these data are taken from Ref. 1. The full energy gap $2\Delta_0$ of Sn has a value of 14 K.

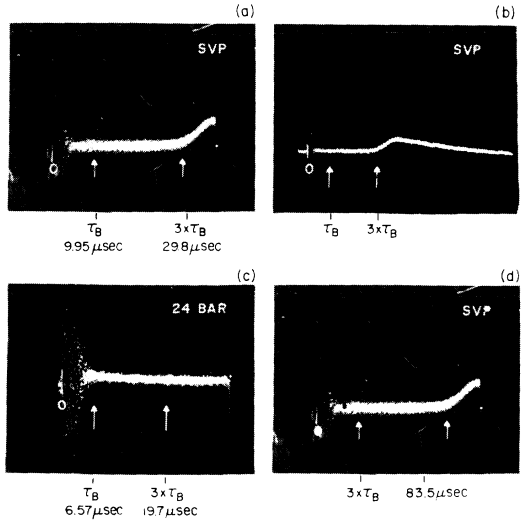

FIG. 3. Tunnel-junction detector signal as a function of time on two time scales and for two pressures. The time of expected arrival for low-frequency phonons is labeled τ_B, the echo time $3\times\tau_B$. At low pressures, signal arrives at $3\times\tau_B$ while at higher pressures, the signal arrives later.

Another interesting aspect of these data is that we do indeed detect some arriving excitation, but at a substantially lower velocity. There is, also, a *qualitative* and *quantitative* difference between the signal detected at SVP and that at 24 bar. At 24 bar, we see the peak of the signal arriving 83.5 μsec after the original pulse and this is the mode that we previously identified[10] as a collective mode in the roton gas (roton second sound). Our detector is merely detecting the upper energy components ($\hbar\omega > 2\Delta_0$) of this collective mode. The temperature and power (variation of the number of rotons) dependences qualitatively bear this out. At SVP, however, the situation is quite different. The leading edge of the detected pulse arrives, to within our accuracy, precisely at $3\times\tau_B$, the time expected for the first echo of the low-frequency phonons generated (but not detected at τ_B). At 24 bar, no signal at $3\times\tau_B$ is detected. In addition the line shapes of the two signals are qualitatively different. The signal at 24 bar has the derivativelike shape (negative overshoot) reminiscent of second sound[6] in other systems. At SVP, however, the pulse shape is very similar to that obtained for ballistic phonons[10] in earlier measurements. In addition, the leading-edge position (at $3\times\tau_B$) does not change with varying power or energy dissipation in the generator, while the velocity of the signal at 24 bar is strongly power dependent.

Since we ascribe the signal at 24 bar to roton second sound, it seems natural to make the same assignment at SVP. There are, however, contradictions associated with this assignment. The velocity is incorrect, for example, and the arrival time at exactly $3\times\tau_B$ suggests that the phonons play some role. The velocity is also not correct for ballistic rotons, as is evidenced by Fig. 2, and an alternate explanation must be found. It is also worth noting at this stage that as a function of pressure the signal that arrives at $3\times\tau_B$ at SVP continuously evolves into the roton second sound at 24 bar so that any explanation of the signal at SVP must include, in addition to the phonons, the rotons in the system.

It is also interesting to note that at the full energy gap $2\Delta_0$ we do not detect any highly dispersed phonons ($v_g \ll c_0$). This is not too surprising since we are near the maximum of the phonon branch, where the group velocity is near zero. In addition, the density of roton states is considerably higher than those for phonons and, finally, at these short wavelengths the scattering of a high-energy phonon with a thermal one (via a four-phonon process) may become sufficiently strong. The calculated value of the mean free path depends on the dispersion parameters assumed.[12] Our data indicate that the mean free path must be less than 1 mm for phonons in the energy range 11–14 K at $T \gtrsim 0.1$ K.

To study the signal at $3\times\tau_B$ relative to the phonon signal, a series of measurements with different fields and hence different sensitivity ranges (see Fig. 1) was performed at a pressure of 2 bar. Some representative curves taken from this series are shown in Fig. 4. Several points are worth noting. As the field is increased, a signal corresponding to ballistic phonons is observed to increase relative to that arriving at $3\times\tau_B$. This result is expected as the energy threshold of the detector sensitivity is reduced and the lower-energy phonons which do propagate these distances[3] are observed. There is an added complication here since at these low pressures the phonons, because of upward dispersion, are susceptible to decay via the three-phonon process, but the qualitative observation of the increase of this signal with increasing H relative to the one at $3\times\tau_B$ is still consistent. Finally, just below the critical field the observed signal is not dissimilar to

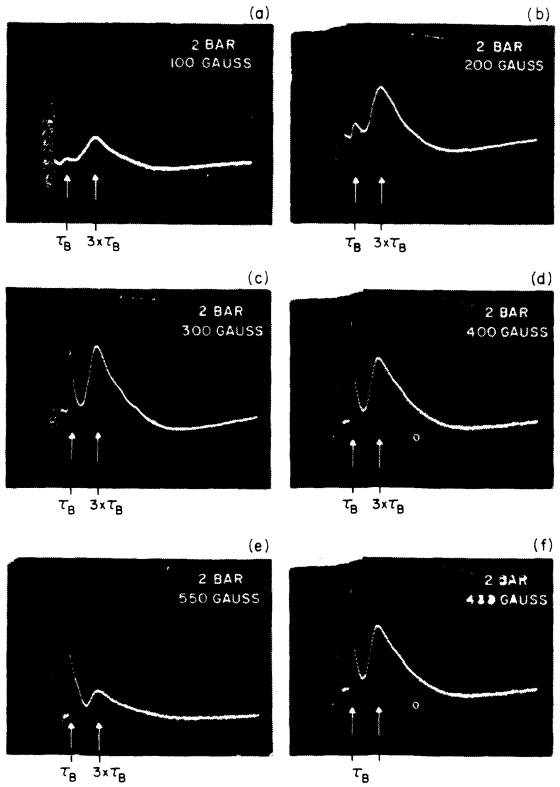

FIG. 4. Detector signal as a function of time for various applied magnetic fields. Pressure is 2 bar. As $\Delta(H)$ decreases, the phonon signal at τ_B increases relative to the signal at $3\times\tau_B$.

that observed in the heat-pulse measurements,[10] which are broad band in nature. A very strong ballistic-phonon signal and a very weak echo (arriving at $3\times\tau_B$) are observed. Although it is not evident on these photographs, as we tune the gap down in energy, we see some dispersion in the arriving ballistic phonons, which we estimate to have an energy of ~10 to 11 K. With increasing field (decreasing Δ) this pulse speeds up. The arrival time of the pulse at $3\times\tau_B$, on the other hand, does not change. Only the strength of this signal relative to the phonon pulse changes.

Another variable available to investigate these phenomena is that of power or energy dissipated in the pulse. By increasing the power dissipated in the generator, the instantaneous temperature is increased and the ratio of rotons/phonons generated will increase. What exactly is the temperature of the pulse is a subtle question which will be deferred to a later section. Qualitatively though, increasing the roton/phonon ratio must have a strong influence on signals we ascribe to either roton second sound or to a phonon roton interaction. Some representative data for 1 and 24 bar at various powers and a field $H=400$ G are illustrated in Figs. 5(a)–5(h). The data are presented in terms of energy dissipation per mm^2 and the pulse width was 0.25 μsec. In Figs. 5(a)–5(d), we see that at relatively low energies the signal is almost exclusively due to ballistic propagating phonons. With increasing energy, what appears to be the echo, arriving at $3\times\tau_B$, grows in strength relative to this phonon pulse. These data suggest that this "echo" signal is indeed dependent upon the excited roton density, which is increasing here relative to the phonon density. The arrival time of this signal (at $3\times\tau_B$) is not power dependent and to within our accuracy is coincident with the arrival of the first echo of the phonon pulse.

At 24 bar, another complication arises. As is shown in Figs. 5(e)–5(h), at low energies the results are not dissimilar to those at 1 bar. However, as we increase the energy dissipated we find, in addition to the signal we ascribed to roton second sound increasing in velocity with increasing energy, another signal, at times intermediate to the phonons and rotons. This signal apparently grows from the echo position and does retard in time with increasing power. This is not observed when $H=0$ but increases with decreasing $\Delta(H)$.

Finally, as a function of energy at even higher energies, we do finally observe at SVP the roton second sound. This is illustrated in Fig. 6, where we show a series of traces at $H=0$ and SVP of the signal obtained for even higher energies. At 3.4 ergs/mm^2 we observe the pulse arriving at $3\times\tau_B$, but with increasing energy, a second peak speeding up with increasing energy rises until it dominates and the $3\times\tau_B$ signal becomes very weak. It appears from these data that the signal at $3\times\tau_B$ attenuates as the roton second-sound amplitude increases. This will be explained in Sec. III as the scattering of phonons as they pass through the cloud of rotons in the roton second sound.

The other variable that one has control of in this experiment is temperature. As was shown earlier[10] at high pressures increasing temperature increases the roton density and roton second sound becomes better defined. Finally, the roton-phonon scattering rate increases to the point

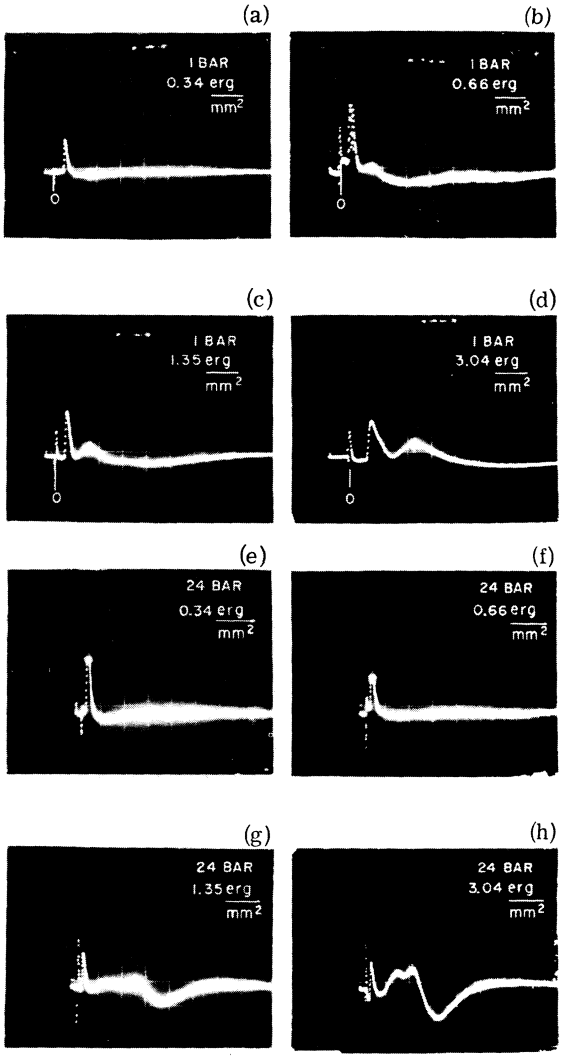

FIG. 5. (a)–(d): Detector signal for various generator energy dissipations. Pressure is 1 bar and the applied magnetic field is 400 G. (e)–(h): Detector signal for various generator energy dissipations. Pressure is 24 bar and the applied magnetic field is 400 G.

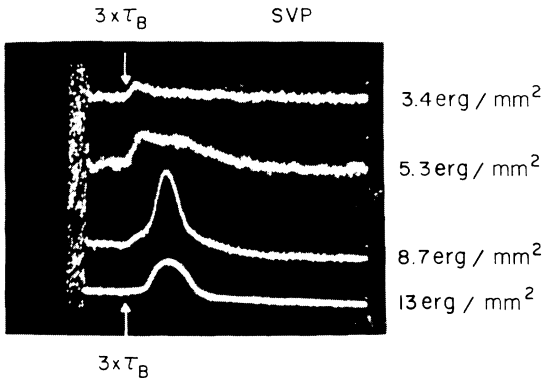

FIG. 6. Detector signal at SVP and low magnetic fields for higher-energy dissipations. At the highest energies, the signal at $3\times\tau_B$ is suppressed and the driven roton second-sound signal dominates.

where the phonon mean free path becomes sufficiently short and the phonons join the second-sound pulse, resulting in second sound in the entire gas of excitations. This is illustrated in Fig. 7, where we show, for $H=300$ G and 15 bar, the temperature dependence of the signal. At 0.12 K we observe the ballistic phonons as well as the roton signal and the intermediate signal of Fig. 5. Raising the temperature, we see, as expected, a sharper, more well-defined roton second sound separate from the ballistic phonons arriving at τ_B. At an even high temperature (0.75 K) the phonons scatter with the rotons and by 1 K complete second sound in the entire gas of excitations propagates.

Because of the confusing wealth of data presented in this section, it is perhaps useful to review the salient features. In particular it is important to recognize the central results that any model describing these data must explain. First, and most important, at SVP with no applied magnetic field, the detected signal arrives at exactly $3\times\tau_B$ while no signal is observed at τ_B. This is contrasted with the data at 24 bar, where the signal velocity is power dependent and arrives substantially later (see Fig. 3). In addition the signal strength increases with energy dissipated more rapidly than the phonon signal with H applied, suggesting a roton nature for the signal. As 2Δ decreases the ratio of phonon signal to "$3\times\tau_B$ signal" increases (Fig. 4). Finally, at high pressures and intermediate fields, in addition to the roton second-sound pulse, an additional signal is observed intermediate to the ballistic phonons and the roton pulse. These pulses, which we generally refer to as "roton" pulses, become better defined roton second sound at higher temperatures.

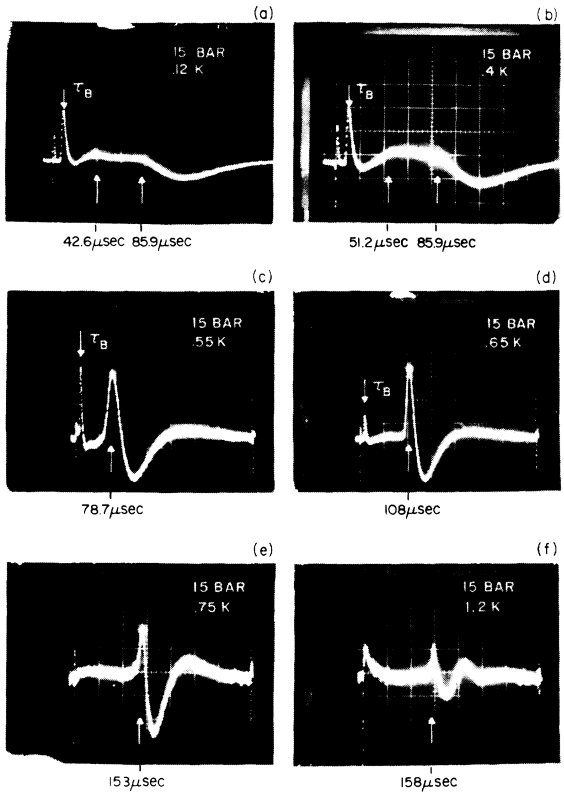

FIG. 7. Temperature dependence of the received signal at 15 bar and 300 G. Note that at higher temperatures, the signal ascribed to roton second sound sharpens and becomes well defined. At even larger temperatures (> 0.75 K) the phonon-roton scattering becomes important and ballistic phonons are no longer observed. The propagating mode is complete second sound.

III. MODEL FOR EXPERIMENTAL RESULTS

We have previously shown[10] that at high pressures (24 bar), in addition to ballistic-phonon propagation at intermediate temperatures, roton second sound is observed. From earlier heat-pulse measurements, a second signal similar to that shown in Fig. 7 for 15 bar has been identified as an interacting roton collective mode. From Khalatnikov and Chernikova,[12] we know that the roton-roton scattering rate can be given approximately by

$$\frac{1}{\tau_{rr}} = \frac{4P_0\mu|V_0|^2}{\hbar^4} N_r , \tag{1}$$

where P_0 is momentum at the roton minimum, and μ is the roton effective mass; the roton potential interaction is of the form $V_0\delta(r)$ and N_r is the roton number density. $|V_0|^2$ is found to be of the order of 4×10^{-76} erg cm^{-3}. A simple estimate of the sensitivity of the detector junctions

suggests that once the rotons are excited either thermally or by the generator in sufficient numbers for detection ($\sim 10^{16}/\mathrm{cm}^3$) their lifetime is short enough to cause roton-roton scattering in the pulse width. This implies that detection of ballistic rotons is not likely using this technique. It should be emphasized, however, that unlike previous heat-pulse[6] measurements, where small excursions from ambient temperature were sought, in this case, large energy dissipations imply large temperature excursions and the concept of interactions with thermal excitations is not valid. The pulse we label as roton second sound is in fact a driven mode whose velocity is strongly dependent upon power and temperature, as was shown previously.[10] As the pulse propagates through the cooler liquid, the roton density dilutes and the pulse broadens. This dilution and broadening is the reason that echos of this driven mode are not observed. Also, with increasing ambient temperature the pulse narrows (see Fig. 7) owing to the fact that for the same energy dissipation, the difference between the pulse and ambient temperatures decreases (because the specific heat is nonlinear in T) and the mode becomes better defined.

The question of the density of injected rotons and phonons is a subtle one. It has been shown previously, in the case of heat pulses in solids,[9] that the "effective temperature" of the pulse can be related to the power dissipated in the heater via the relation

$$\frac{P}{A} = \bar{v}\rho \int_{T_A}^{T_h} C_v(T)\, dT\,, \tag{2}$$

where P/A is the power per unit area dissipated, $\bar{v}$ is the average velocity of the excitations created, ρ is the density of the medium, C_v is the specific heat, and T_A and T_h are the ambient and heater temperatures, respectively. This relation is derived using a blackbody assumption, i.e., thermal equilibrium inside the pulse while it is on. Within the framework of these assumptions, we can estimate T_h and hence the phonon and roton density launched. There is a problem associated with the choice of the parameter $\bar{v}$ in this expression as the velocities of the various components are quite different, and in fact temperature dependent as measured previously.[6] We then slightly modify (2) to

$$\frac{P}{A} = \rho \int_{T_A}^{T_h} \bar{v}(T) C_v(T)\, dT\,. \tag{3}$$

We then choose our previously estimated values of $\bar{v}(T)$ and calculate the final heater temperatures of a function of dissipated power. Those estimates for SVP and 24 bar are shown in Fig. 8, where we again emphasize that a blackbody or equilibrium approximation inside the pulse is assumed. T_A is assumed to be 0.1 K for these calculations, and C_v was numerically determined from measured $E(k)$ relations[1] and agree to within a few percent with measured values. This curve illustrates clearly the profound difference in roton density for the same power dissipations at SVP and 24 bar. For example, for a power of 2 $\mathrm{W/cm}^2$, the roton density at 24 bar and SVP is, respectively, 1×10^{18} and $1.4\times10^{15}/\mathrm{cm}^3$. At 30 $\mathrm{W/cm}^2$, the roton densities are 2×10^{19} and $1\times10^{19}/\mathrm{cm}^3$. It was estimated earlier that the junction sensitivity was such that 10^{16} rotons/cm^3 should be detected, while here we are suggesting that the number density at the generator is $\sim 10^{19}$. This difference is due to two reasons. First, there is a geometric spatial dilution of approximately one order of magnitude in transit across the He II. In addition, because there is a broadening of the pulse in time by about two orders of magnitude, the arriving roton signal does indeed have a density $\sim 10^{16}/\mathrm{cm}^3$. It is evident, then, that in this power range there are considerably more rotons launched at 24 bars then at SVP, particularly at low powers, and consequently the roton signal is observed under higher pressures at lower powers.

These model calculations suggest that for the powers dissipated in this experiment, the instantaneous heater temperature is somewhere in the vicinity of 0.8 to 1.0 K. This number appears somewhat high and so the assumptions made to derive Fig. 8 should be reviewed. First, it was assumed that the source was blackbody in nature and the pulse was in thermal equilibrium while on. This seems justified in view of the values obtained for the effective temperature as the individual excitations are short lived at these temperatures. It

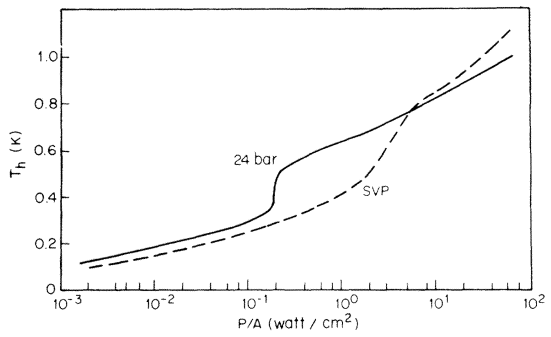

FIG. 8. Calculated values for the generator temperature at two pressure as a function of power dissipation. These curves were calculated from Eq. (3), where the sharp rises reflect the velocity profiles $\bar{v}(T)$.

was also assumed that the specific heat in the entire system was dominated by the He. The generators were evaporated on fused-glass substrates whose specific heat is negligible compared with He II at these temperatures. We do not expect the estimates in Fig. 8 of the generator temperatures to be in gross error because of the assumptions made on the average velocity since it is seen that a change in $\bar{v}(T)$ of even a factor of 2 will change T_h by $\lesssim 10\%$ and so these estimates are probably reliable within this uncertainty.

In view of this discussion, from the estimates of roton density and $1/\tau_{rr}$ from Eq. (1), it is safe to assume that any rotons launched in these experiments will be interacting strongly and the explanation of the signal observed in Fig. 3 at 24 bar as a driven roton collective mode seems valid. In thermal equilibrium (small temperature excursions from T_A) this would be roton second sound. We emphasize that Eq. (1) can be strongly modified for rotons with momentum away from P_0. Also, this problem of roton-roton scattering has been more extensively treated in connection with estimates of the two-roton binding energy[5] but the value for $1/\tau_{rr}$ is not severely altered.

At low pressures, the situation is somewhat different. The results of Fig. 3 indicate that the signal arrives at a time which is exactly $3\times\tau_B$, i.e., the arrival time for the first echo of the ballistic phonon pulse. As indicated earlier, the evidence suggests that this signal must be related to both the arrival of phonons *and* rotons. To explain this result, we invoke a scattering process first suggested by Pitaevskii.[8] From inelastic neutron scattering data[1] (Fig. 2) at SVP it appears that there is a region of the roton branch where the group velocity of the rotons reaches the sound velocity. At and above this threshold point $F_c(k_c)$, rotons can spontaneously decay into a phonon and a roton, i.e.,

$$\text{roton} \rightarrow \text{phonon} + \text{roton}\,. \tag{4}$$

Energy and momentum can be conserved in this collinear process and the decay rate was calculated by Jackle and Kehr[11] to be

$$\frac{1}{\tau_r} = \frac{\hbar k_c^3 |k - k_c|^2}{24\pi\rho}\,. \tag{5}$$

For any realistic parameters we choose from the excitation spectrum ($k_c = 2.13$ Å^{-1}, $|k - k_c| = 0.15$ Å^{-1}), we find that rotons are extremely short-lived in this region of k space and decay via this process. The inverse process, the elevation of a roton via the absorption of a low-energy phonon,

$$\text{phonon} + \text{roton} \rightarrow \text{roton}\,, \tag{6}$$

was also calculated by Jackle and Kehr and the absorption rate of a phonon of wave vector q was determined to be

$$\frac{1}{\tau_{\text{phonon}}} = \frac{\hbar k_c^4 q}{8\pi\rho}\, e^{-E_c(k_c)/kT}\,. \tag{7}$$

We propose, then, the following model for the signal observed at $3\times\tau_B$ at SVP. When the pulse is launched, both phonons and rotons are created; the numbers of each can be determined from Fig. 8 and specific-heat considerations. Because of their higher velocity, the phonons escape the interacting roton cloud and propagate ballistically to the detector. The phonons are not detected because their energies $h\omega < 2\Delta_0$, as described earlier. The phonons are then reflected, pass through through the roton cloud, are reflected by the generator, and propagate back toward the detector. Approaching the detector, the phonons again overtake the roton cloud and the collinear process (6) can occur at a rate given by Eq. (7). This process elevates a roton of energy $E_c(k_c) \rightarrow E_c(k_c) + c_0 q$. If $E_c(k_c) + c_0 q > 2\Delta_0$ it is detected.

This model qualitatively describes the results observed. First, the coincidence of a roton cloud with a phonon cloud in the region of the detector is necessary for the elevation of the excitation to $E > 2\Delta_0$. The lifetime of a roton in that state, as estimated from (5), is very short and so the scattering process must occur in the vicinity of the detector. The model also explains why signal is observed at $3\times\tau_B$ at SVP and not at 24 bar. From Fig. 2 it is evident that at 24 bar this three-particle process is not allowed since v_g is always $< c_0$. Thus only the driven roton second-sound mode is detected. At higher powers at SVP (see Fig. 6) both this $3\times\tau_B$ signal from the up conversion of low-energy phonons by high-energy rotons and the roton second sound are detected as a larger density of rotons is generated. Finally, at even higher roton density, the four-particle process

$$\text{phonon} + \text{roton} \rightarrow \text{phonon} + \text{roton} \tag{8}$$

takes over and phonons passing through the roton cloud are scattered out of the beam after the first reflection from the detector, and hence the signal at the highest powers at $3\times\tau_B$ attenuates (Fig. 6). In Sec. IV we will describe experiments to verify this three- and four-component scattering model. In addition we will present estimates of the various scattering rates and at what pressure this Pitaevskii process cuts off.

This qualitative model can also describe the data when the detector energy gap is tuned with magnetic field (Fig. 4). The detector sensitivity is increased for the lower-energy phonons with increasing field and so a pulse representing the

transit time for the phonons at τ_B increases in intensity. Finally, of course, as the detector becomes broad band in its response [Fig. 4(f)], the pulse shape becomes very similar to that previously studied in heat-pulse measurements. At higher pressures with intermediate values of Δ, in addition to the roton pulse, a signal intermediate to the phonons and rotons is also detected which we interpret as the arrival of an echo pulse scattered by the four-particle process. We interpret this as a four-particle process because of the diffusive nature of this pulse (its leading edge is close to $3\times\tau_B$ but the peak is considerably delayed) and its power dependence is characteristic of a noncollinear scattering process. Also, the fact that this "diffuse echo" disappears with increasing temperature is consistent with this interpretation. Again, estimates of this phonon + roton → phonon + roton scattering process will be made in Sec. IV. In summary of this section, we have presented a tentative model based on roton-roton scattering and roton-phonon scattering, which we argue qualitatively describes the data of Sec. II. At high pressures, we show that the generated roton density is higher than at low pressures for the same power or energy dissipation and the signal detected is a driven roton second sound. To explain how this roton mode continuously evolves into a signal arriving at $3\times\tau_B$ at low pressures, we have invoked a rather restrictive three-particle scattering process first suggested by Pitaevskii and implied by inelastic neutron scattering data. In Sec. IV we will describe some experiments to verify this model and some numerical estimates of the strengths of the various scattering processes.

IV. TEST OF MODEL

We have proposed that at SVP the signal arriving at $3\times\tau_B$ [Fig. 3(a)] is a result of the coincident arrival of phonons and rotons and the Pitaevskii three-particle process. This process must turn off as a function of pressure and so a measure of the amplitude of the signal at $3\times\tau_B$ as a function of pressure would indicate when this occurs. We have measured the amplitude of the signal at 3 times the arrival time of the *peak* of the ballistic-phonon signal. A plot of this is shown in Fig. 9. At lower pressures we see a monotonically increasing signal which probably reflects the increasing roton density with increasing pressure for the same power or energy dissipation. In the vicinity of 6 bar, we see a sharp drop in the signal strength until at 10–12 bar it has completely disappeared at $3\times\tau_B$. There is, of course, still signal observed at later times which we ascribe to the driven roton mode. Upon careful inspection of the line shape in this intermediate region between 6 and 12 bar, it is evident that the arriving signal has two components, the phonon-roton pulse at $3\times\tau_B$ and the slower roton second-sound signal. These data are a measure of the pressure range over which the region in phase space where $v_g = c_0$ decreases to zero. It is not at all evident from neutron scattering results that this "pinch off" occurs in this pressure range but these data clearly indicate a scattering threshold at ~6 bar and enhance the plausibility of the model proposed in Sec. III.

A more direct collinear scattering experiment can be performed as a test of the model. This is performed in the following way. A pulse is applied to the generator (the roton pulse) and then ~10 μsec later a second pulse (the phonon pulse) is applied. Phonons from the second pulse must propagate *through* the slower roton cloud before striking the detector. If the detector is magnetically tuned in such a fashion as to sense the arrival of the phonons from the second pulse one can perform a collinear phonon-roton scattering experiment. By varying the energy dissipated in the first pulse, the roton density can be varied and the arriving signal as a function of roton density determined. In Fig. 10 we show a series of traces obtained in this double-pulse experiment for various energies of the first roton pulse P_1. For $P_1 = 0$ we see at a time τ_B after the second pulse the arrival of the ballistic phonons from that pulse. At a later time we see the arrival of the $3\times\tau_B$ signal. As the number of rotons in the roton cloud from the first pulse is increased, we see the attenuation of the ballistic-phonon pulse and only the later roton signal remains. The phonons were evidently scattered by the rotons.

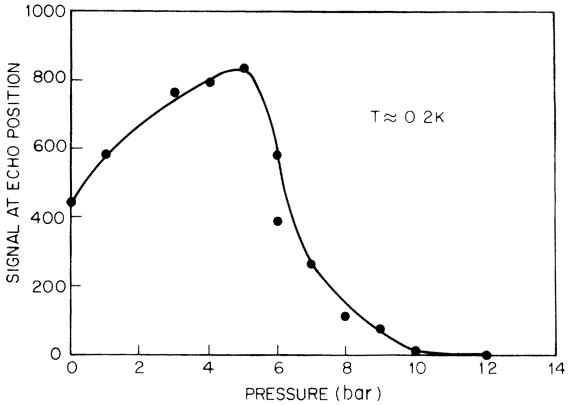

FIG. 9. Signal strength at the echo position of the *peak* in the ballistic-phonon pulse. The drop starting at 6 bar reflects the turnoff of the Pitaevskii process. See text.

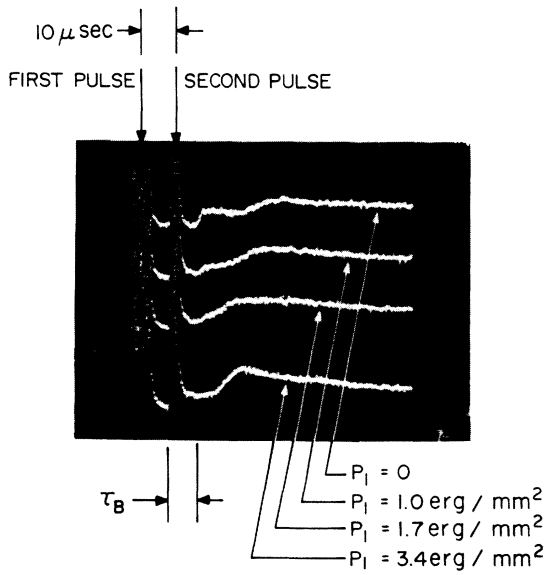

FIG. 10. Detected signal in the double-pulse experiment for various energy dissipations in the first pulse P_1. At $P_1 = 0$ we observe at τ_B after the second pulse the arrival of the ballistic phonons. With increasing roton density (increasing P_1) this signal disappears.

There are, of course, two different scattering mechanisms possible for this apparent phonon-roton scattering process. The more traditional scattering process is that given in Eq. (8), and Khalatnikov and Chernikova[12] have determined a scattering rate for this process given by

$$\frac{1}{\tau_{pr}} = (2\pi)^{17/2}\,\Gamma\left(\frac{k_B^{9/2}}{h^7}\right) \times\left(\frac{P_0^4\,\mu^{1/2}}{\rho^2 c_0^5}\right) T^{9/2} e^{-E_g/k_B T}\,, \tag{9a}$$

where ρ is the density,

$$\Gamma = \tfrac{2}{9} + \tfrac{1}{25}(P_0/\mu c_0)^2 + \tfrac{2}{9}(P_0/\mu c_0)A + A^2\,, \tag{9b}$$

and

$$A = \left(\frac{\rho^2}{P_0 c_0}\right)\frac{\delta^2 E_g}{\delta\rho^2} + \left(\frac{P_0}{\mu c_0}\right)\left(\frac{\rho}{P_0}\,\frac{\delta P_0}{\delta\rho}\right)^2\,. \tag{9c}$$

Here E_g is the roton energy gap.

The other scattering process possible is that given by (6), with a rate given by (7). We can estimate the importance of these two processes with recourse to our blackbody approximations. We can calculate for various temperatures estimated in Fig. 8 and using Eq. (7) and (9) the probability of scattering a phonon via these two processes. We assume thermal equilibrium during the pulse and estimate the scattering rates $1/\tau_{pr}$ from (9) for the four-particle process and $1/\tau_{\text{phonon}}$ from (7). The results of these estimates for various temperature pulses as well as estimates of the transmission probability for each process are given in Table I. Here we choose $E_c = 10.2$ K and $k_c = 2.13$ Å^{-1}. In this calculation we have also considered q values reflecting the temperature of the pulse (the peak in the distribution given by $q = 2.8kT/\hbar c_0$). This is probably a somewhat low estimate of the q values of the propagating phonons, but even for this choice of q we see from Table I that the dominant scattering mechanism is the Pitaevskii or three-particle process. It is also interesting to note that the pulse-temperature range, over which the phonon transmission through the roton cloud goes to zero, is in the range of our earlier estimates of Fig. 8 and gives us confidence in our earlier assumptions. Alternatively, we can consider this measurement as a verification of the estimates of the phonon-roton scattering rate. These estimates also explain the data presented in Fig. 6, where at the very high energies (or generator temperatures) the pulse arriving at $3\times\tau_B$ disappears. This is due to the four-particle scattering of the phonon pulse after reflection as it passes through the roton cloud for the first time. As a result, the only signal observed at the high excitation levels is the driven roton pulse similar to that observed at high pressures.

In addition to varying the roton density in the double-pulse experiment, the pressure can also be adjusted. According to our model and the data of Fig. 9, as a function of pressure this Pitaevskii scattering process should pinch off as the phase space over which $v_g \geq c_0$ goes to zero. When v_g becomes less than c_0, only the four-particle process is possible. The results of an experiment to test this phenomenon are shown in Fig. 11, where we show some representative pulses for various pressures. In each photograph we show a trace derived from the double-pulse experiment in which the first or roton pulse P_1 is either zero or 5.3 erg/mm^2. This experiment was done in an intermediate magnetic field in which the arrival of ballistic phonons was clearly visible, as is evidenced by the lower trace of each photograph. It is clear though, that as the pressure is increased we go from a condition where the ballistic phonon is not observed (scattered) to where it is diffusive in nature (at 5 bar), until by 24 bar it is clearly well defined and propagating ballistically. If we plot the ratio of the amplitude of the pulse at τ_B in this double-pulse experiment to that when $P_1 = 0$ the results are shown in Fig. 12. Here we see a rather sharp change in the signal strength between 8 and 12 bar and we interpret this as the turning off of the Pitaevskii

TABLE I. Estimates of $1/\tau_{pr}$ and $1/\tau_{\text{phonon}}$ as well as the transmission probabilities p of phonons of wave vector q through the roton cloud at SVP.

T pulse (K)	$1/\tau_{pr}$ (sec^{-1})	p_{pr}	$1/\tau_{\text{phonon}}$ (sec^{-1})	p_{phonon}
0.7	9.8×10^{5}	0.94	$0.28q$	0.81
0.8	8.6×10^{6}	0.59	$1.64q$	0.24
0.9	4.9×10^{7}	0.05	$7.12q$	0.00
1.0	2.0×10^{8}	0.00	$22.1q$	0.00

process, consistent with our results of Fig. 7. In fact, inspection of the observed line shapes of Fig. 11 shows clear evidence for the existence of a scattering process turning off between 8 and 12 bar.

We must also estimate the change in the four-particle scattering rate $1/\tau_{pr}$ due to this pressure variation. From Table I we estimate, at SVP for a 0.8-K roton pulse, $1/\tau_{pr}=8.64\times10^{6}$ sec^{-1}, while from Eq. (9), at 24 bar $1/\tau_{pr}=4.76\times10^{6}$ sec^{-1}. We see then, for the same temperature, a change in the scattering rate by a factor of approximately 2 throughout the pressure range and we interpret the gradual over-all change in Fig. 12 as reflecting this slow change in the scattering rate due to this process. The situation is certainly complicated by the fact that the two phonon-roton scattering processes are comparable at SVP but a precipitous change in the vicinity of 8–10 bar is not expected for the four-particle process while such an effect is indeed expected for the Pitaevskii process.

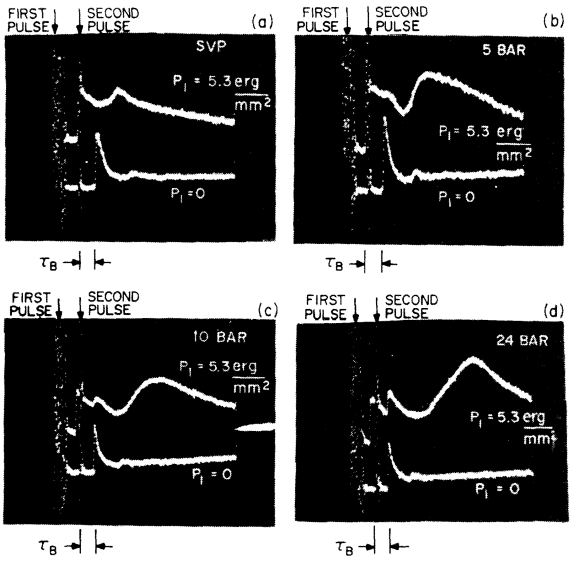

FIG. 11. Pressure dependence of the ballistic-phonon signal for a given power dissipation in the first pulse (roton pulse). At SVP, no ballistic phonon at τ_B is observed. At 24 bar it is clearly resolved.

Finally, we can interpret the intermediate pulse observed at high pressures [Figs. 5(a)–5(d)] as a diffuse echo of the propagating phonons. With increasing energy dissipated this pulse retards in time becoming more diffusive in nature with increasing roton density. The phonons must pass through the roton cloud twice before arriving as an echo and in that way can scatter via the four-particle process. We recall that this signal is not observed when the detector threshold is not reduced by an applied field and hence this excitation is of lower energy.

V. CONCLUSIONS

Using superconducting Sn phonon fluorescent sources and tunnel-junction detectors, we have studied the propagation properties of high-frequency excitations in He II at low temperatures. With the detector sensitive only to excitations $h\omega>14.0$ K, at SVP we find a signal arriving at a time corresponding to the arrival of the first echo of phonons traveling at the sound velocity c_0. At higher pressures, the signal retards in time and the arrival time becomes dependent upon energy dissipated in the generator. We

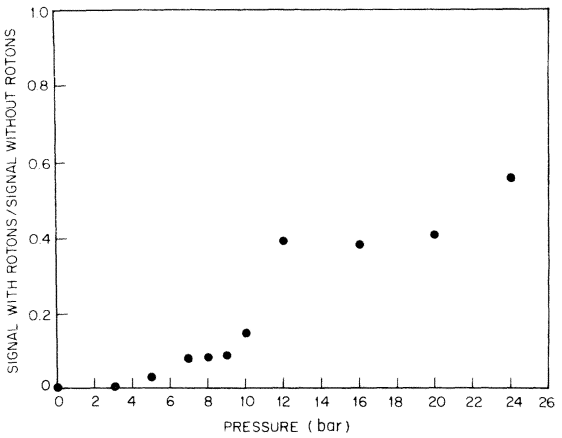

FIG. 12. Ratio of ballistic-phonon signal strengths with and without roton pulse. These points are the ratios of the signal at τ_B after the second pulse taken from the data of Fig. 11.

ascribe this behavior to two separate phenomena. At low pressures, we believe the signal is due to the simultaneous arrival of the phonon echo and a roton cloud. Invoking a scattering process suggested first by Pitaevskii we explain why the signal arrives at $3\times\tau_B$. With increasing pressure this scattering turns off in the pressure region 6–12 bar and the signal at $3\times\tau_B$ disappears. At higher pressures we interpret the arriving signal as a driven roton second-sound mode.

Numerical estimates are made of the various phonon-roton scattering rates and these estimates are consistent with this interpretation. In particular, it is found that at SVP for a generator temperature of 0.7 to 0.8 K the dominant scattering process for phonons is this Pitaevskii three-particle process. At higher pressures, it is found that this process turns off, presumably as the group velocity of the fast-roton region becomes less than the sound velocity. Precise inelastic neutron scattering measurements in the pressure region indicated by this work would be interesting as the model and experiments predict that v_g drops below c_0 in this range.

ACKNOWLEDGMENTS

We would like to thank J. P. Garno and M. A. Chin for their expert technical assistance.

[1]For a review, see A. D. B. Woods and R. A. Cowley, Rep. Prog. Phys. 36, 1135 (1973).
[2]H. J. Maris, Phys. Rev. A 8, 2629 (1973); 7, 2074 (1973); 9, 1412 (1974).
[3]R. C. Dynes and V. Narayanamurti, Phys. Rev. B 12, 1720 (1975).
[4]R. L. Woerner and T. J. Greytak, J. Low Temp. Phys. 13, 149 (1973).
[5]J. Solana, V. Celli, J. Ruvalds, I. Tüttö, and A. Zawadowski, Phys. Rev. A 6, 1665 (1972).
[6]V. Narayanamurti, R. C. Dynes, and K. Andres, Phys. Rev. B 11, 2500 (1975).
[7]E. H. Graf, V. J. Minkiewicz, H. B. Moller, and L. Passell, Phys. Rev. A 10, 1748 (1974).
[8]L. P. Pitaevskii, Zh. Eksp. Teor. Fiz. 36, 1168 (1959) [Sov. Phys.–JETP 9, 830 (1959)].
[9]R. C. Dynes and V. Narayanamurti, Phys. Rev. B 6, 143 (1972).
[10]R. C. Dynes, V. Narayanamurti, and K. Andres, Phys. Rev. Lett. 30, 1129 (1973).
[11]J. Jackle and K. Kehr, Phys. Kondens. Mater. 16, 265 (1973).
[12]I. M. Khalatnikov and D. M. Chernikova, Zh. Eksp. Teor. Fiz. 49, 1957 (1965) [Sov. Phys.–JETP 22, 1336 (1966)].

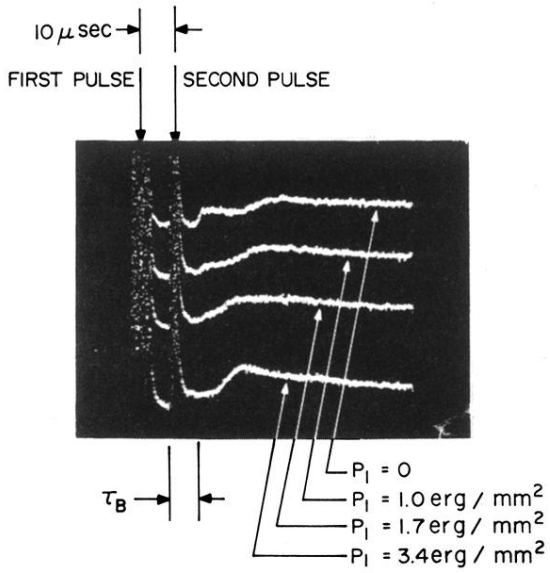

FIG. 10. Detected signal in the double-pulse experiment for various energy dissipations in the first pulse P_1. At $P_1=0$ we observe at τ_B after the second pulse the arrival of the ballistic phonons. With increasing roton density (increasing P_1) this signal disappears.

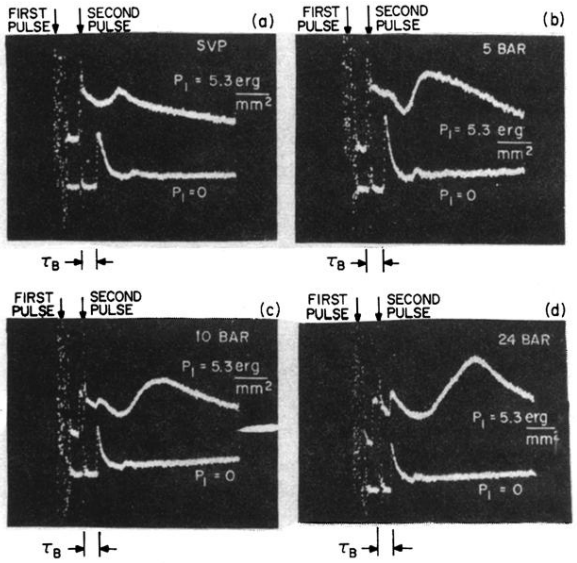

FIG. 11. Pressure dependence of the ballistic-phonon signal for a given power dissipation in the first pulse (roton pulse). At SVP, no ballistic phonon at τ_B is observed. At 24 bar it is clearly resolved.

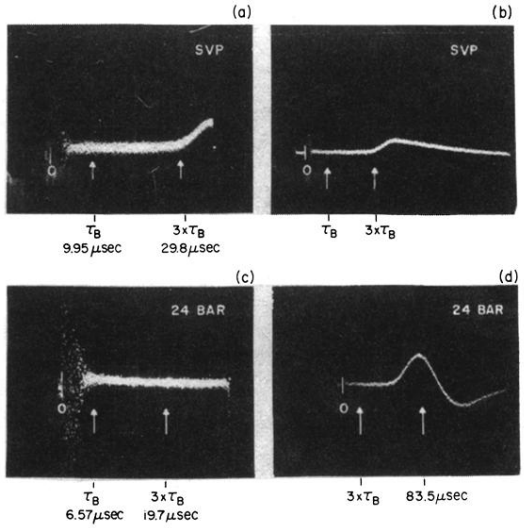

FIG. 3. Tunnel-junction detector signal as a function of time on two time scales and for two pressures. The time of expected arrival for low-frequency phonons is labeled τ_B, the echo time $3 \times \tau_B$. At low pressures, signal arrives at $3 \times \tau_B$ while at higher pressures, the signal arrives later.

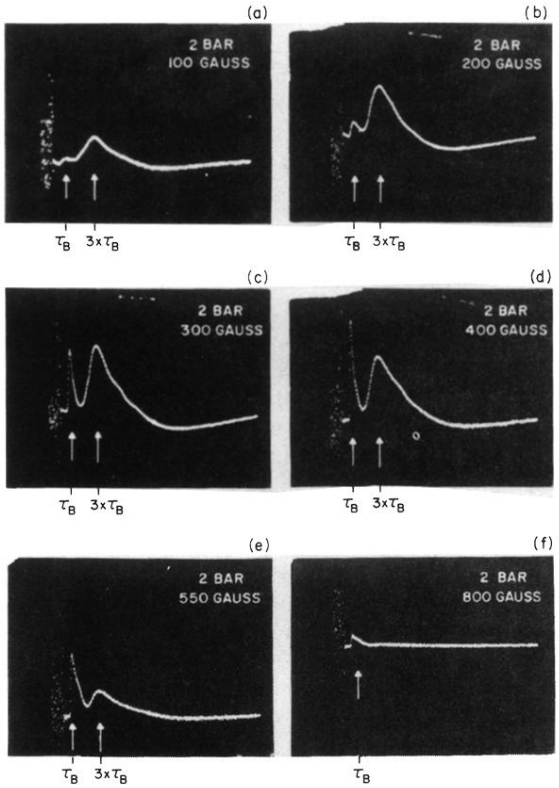

FIG. 4. Detector signal as a function of time for various applied magnetic fields. Pressure is 2 bar. As $\Delta(H)$ decreases, the phonon signal at τ_B increases relative to the signal at $3\times\tau_B$.

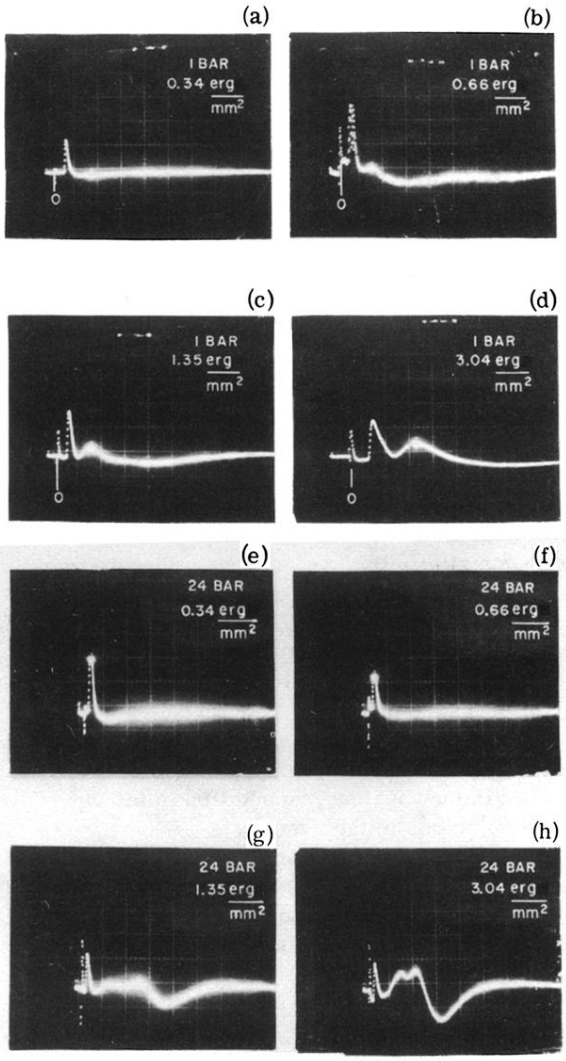

FIG. 5. (a)–(d): Detector signal for various generator energy dissipations. Pressure is 1 bar and the applied magnetic field is 400 G. (e)–(h): Detector signal for various generator energy dissipations. Pressure is 24 bar and the applied magnetic field is 400 G.

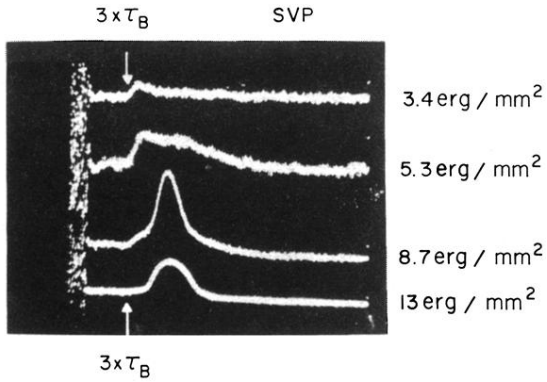

FIG. 6. Detector signal at SVP and low magnetic fields for higher-energy dissipations. At the highest energies, the signal at $3\times\tau_B$ is suppressed and the driven roton second-sound signal dominates.

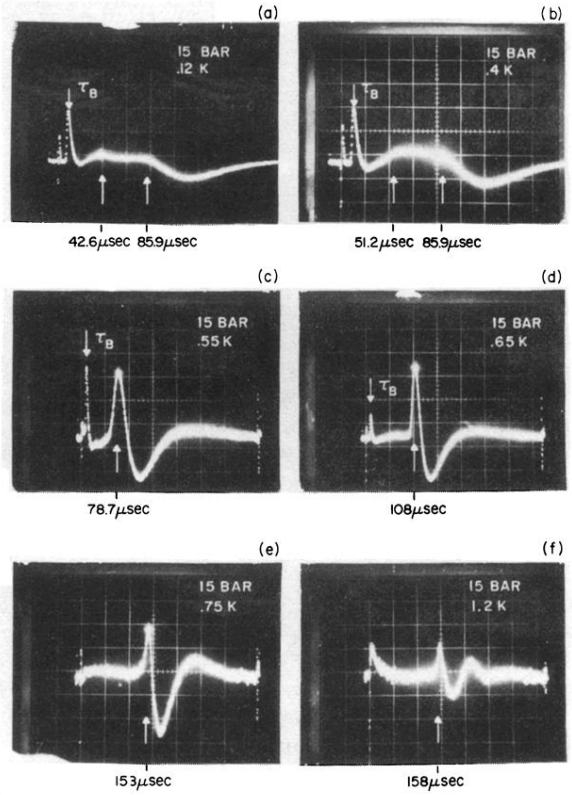

FIG. 7. Temperature dependence of the received signal at 15 bar and 300 G. Note that at higher temperatures, the signal ascribed to roton second sound sharpens and becomes well defined. At even larger temperatures (> 0.75 K) the phonon-roton scattering becomes important and ballistic phonons are no longer observed. The propagating mode is complete second sound.